Study of the factors limiting the Q factors of high performance quartz resonators.

Jacques Detaint, Bernard Capelle, Yves Epelboin.

Institut de Minéralogie et de Physique des Milieux Condensés (IMPMC), UMR 7590 CNRS. Universités Paris VI, Paris VII et INPG. 140, rue de Lourmel ; 75015 Paris. France.

***Abstract*—In this contribution we review the main origins of dissipation in crystal resonators. Several factors appear to be important: the intrinsic dissipations (viscous losses, the dielectric losses and the conductivity), the leakage of acoustical energy via the fixations and the energy dissipation resulting of the existence of other modes, more dissipative (electrical interactions). A calculation is made of the influence of intrinsic dissipation in energy trapping resonators.**

I. INTRODUCTION

Although the synthetic quartz material has been greatly improved in the past 30 years (impurity content, including OH concentration, density of extended defects, etc…), the Q factors of the most performing quartz resonators were not very significantly improved during this period; so that several questions remain about the origin of the limitation of the Q factors. The purpose of this paper is to examine this situation using experimental and computed results to discuss the possible phenomena limiting the performances. The limiting factor the most often considered is constituted by the intrinsic acoustic losses of quartz and eventually of the electrodes. Following the experimental results obtained by Warner [1], it is frequently considered that several kinds of well-designed high performance resonators (5^{th} overtone plane resonators, and overtone plano-convex resonators) have losses, which are approaching very closely a value intrinsic to the material (for the considered frequency, orientation and mode). The one dimensional computation that have been made recently or some times ago [2 to 8] have given results which are generally considered as compatible with the analysis of Warner.

A factor which is very important in many cases, and that can be suspected directly or indirectly, even in the case of high performance resonators, is constituted by the energy leakage outside of the resonator via the mounting clips (dissipative boundary conditions). We have observed that this phenomenon was present in all the fundamental mode resonators studied and that it is quite certainly at the origin of the limitation of the Q factor of most of the fundamental mode devices. We will present several observations concerning these phenomena and discuss the sensibility of the detection method used to study it (stroboscopic topography). Other phenomena will be then discussed such as the influence of stationary coupled modes, the electrical interactions between modes (all the modes are more or less excited in devices submitted to forced vibration by an electrical signal even if this one has a perfect spectral purity). The electrical interactions are very important in devices using materials with a high coupling factor, but they cannot be neglected for quartz since modes relatively close to the used one can have significantly higher losses and so affect the useful mode. We will then present a computation made to better understand the effect of the acoustic losses and of conductivity in energy trapping resonators.

A. experimental observations

1) Progressive modes dissipating energy though the mounting structure

It was often observed that the Q factor of very high performance resonators (third or fifth overtone plane or plano-convex resonators) is dependent of the mounting structure. If the same plate is mounted several times on different supports, a noticeable dispersion of the measured Q factor is observed. This dispersion (typically of the order of 5%) is of comparable magnitude as that observed in a batch of resonators fabricated with the same high quality material. This seems to indicate that sensitivity to fixation conditions exists and that some energy dissipation via the fixation may exist. *In the case of fundamental mode devices, we have observed [9-to 11] that all the examined plane thickness shear resonators, employing any material, display progressives modes* that are certainly at the origin of a limitation of the Q factors to a value much smaller than the intrinsic dissipation. For AT quartz, the measured values for the fundamental of plane resonators is generally quartz below 1.10^5, but it can reach some how higher values with bevelled resonators and it is most often much smaller with miniaturized devices. In other materials, the Q factors of fundamental mode resonators are often lower than in quartz, this is particularly the case for near X-cut lithium tantalate. In figure 1, we recall the observations made

978-1-4244-3510-4/09/$25.00 ©2009 IEEE

on a fundamental mode quartz crystal (6.338560 MHz) made using a quite large flat plate (15mm diameter).

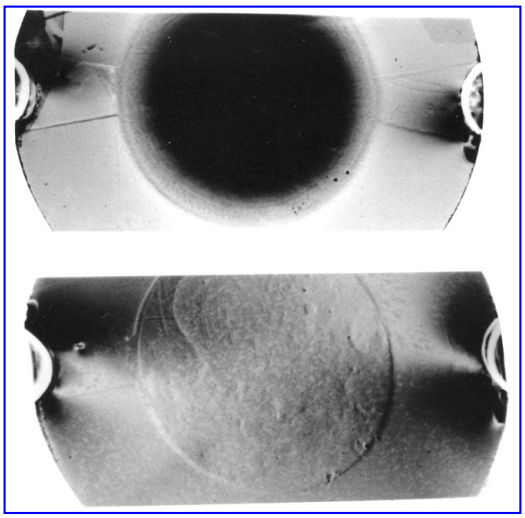

Figure 1. Time integrated topographs displaying only the stationary component (u_1 upper image, u_3 lower image),

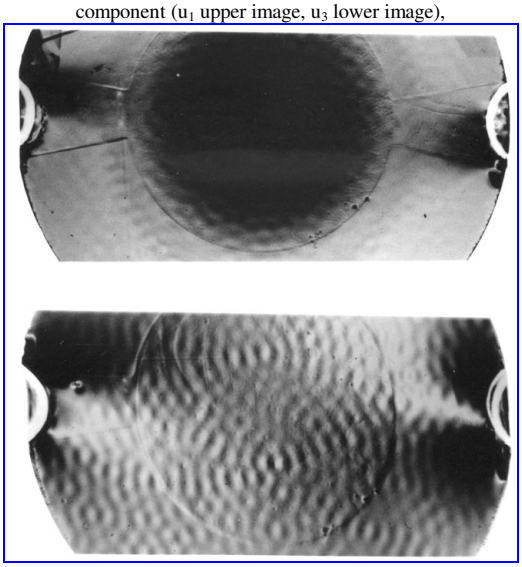

Figure 2. Time resolved image displaying both the stationary and the progressive components. There are a u_1 and a u_3 progressive component.

The progressive modes are imaged using stroboscopic topography; they are easily characterized by the fact that they disappear in a density of grey in the time-integrated topographs. In the case of figure 1 the progressive mode appears to have u1 and u3 components while the main component of the stationary mode has practically only an u_1 component. True stroboscopic observations were made using a slowly and continuously variable phase between the excitation signal and the recurrent pulse of synchrotron radiations and using a high-resolution x-ray camera and a video recorder to capture a motion picture of the diffraction images. They have shown, in all cases, a large ratio of standing wave in the progressive components. These ones are created near the centre of the device and progresses towards the fixation of the resonator in a complex manner. These experiments have shown that only a small fraction of the stored energy of the progressive wave is in fact conducted towards the mounting clips in a given time (In figures 1 and 2, it is practically the amplitude of the displacement that is imaged). This has allowed estimating that the ratio of the stored energy (mostly constituted by the u_1 component of the time integrated topography) to the energy conducted to the mounting clips per second was of an order of magnitude compatible with the measured Q factor of the resonators.

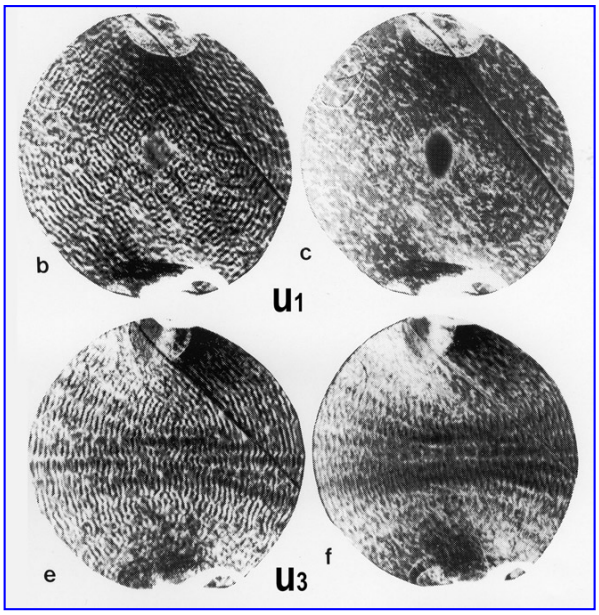

Figure 3. Progressive waves in X-cut litum tantalate resonators (c,f - time integrated, b,e time resolved)

Figure 3 presents typical observations made in lithium tantalate resonators (fundamental fast shear mode 31.69280 MHz). The progressive components are much more intense and it exists here a stationary u_3 component (u_1 is taken as the projection of the 1D. fast shear displacement on the plane of the plate). Although, in each case, the exact shape depends on the relative phase between the excitation current and the X-ray pulses used to produce the image, many very different shapes were observed for the progressive components of the different resonator studied. Most often, their shape is very intricate and very variable between the different resonators even with practically identical units.

Detection limit: The limit of detection of the progressive (as of the stationary) components, in terms of displacement, is presently of the order of some tenth of angstrom, depending on the experimental conditions (X-ray wave length, thickness, diffraction vector, etc…) [10]. Most probably, this does not allow to detect progressive waves in high performance resonators whose Q factors are approaching those considered as being close to the limit due to the intrinsic losses of quartz (at least in the frequency range 4 to 12MHz where the experiments were made with quartz).

B. Stationay "coupled modes".

Such "plate mode" components are very frequent in the thickness modes resonators, and particularly in miniaturized devices. In many cases, they extend up to the fixations and are suspected to conduct energy outside of the devices, may be via undetected progressive waves or by another unknown mechanism. The "coupled modes" related to the activity dips were identified at several instances as having, plate mode type, stationary components extending largely across the resonators. Often the resonators presenting such components have lower Q factors than the other ones in the same batch.

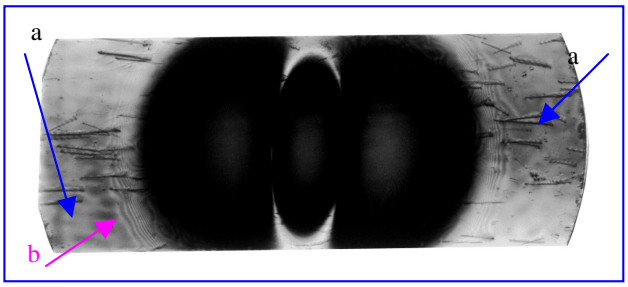

Figure 4. Evidence of "coupled modes" (a) in a high Q resonator (anharmonic mode) and fringes of equal displacement (b) (the 1st one appears for u_1=some 0.1 Å).

In figure 4, we can observe coupled modes occurring in the external region of a high Q plano-convex resonator.

C. Electrical coupling of all the forced modes.

As most distributed components, the crystal resonators have an equivalent scheme generally constituted of infinity of motional arms, each representing a vibration mode.

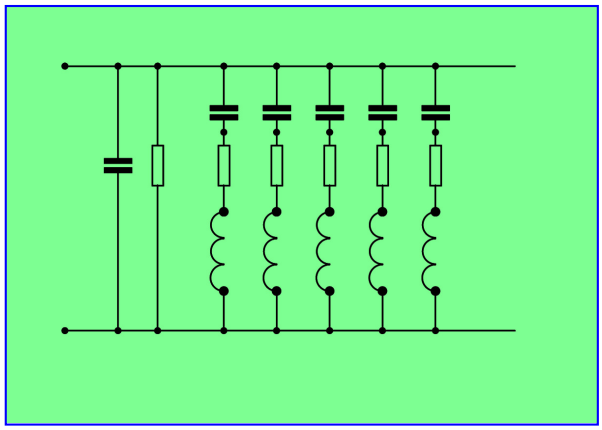

Figure 5. Equivalent scheme of a resonator presenting viscous damping and conductivity (or/and dielectric losses).

The losses corresponding to one mode (fn) are usually represented by a serial resistance in the corresponding RLC circuit. They contribute more or less to the non-reactive part of the admittance near any other resonance frequency (fp) of the device in a manner that is an intricate function of fp-fn and of the values of the other elements of the equivalent scheme. It is frequent that anharmonic modes having resonance frequencies close to that of a mode used to make a high performance resonator have large extensions in the plate and much higher losses and so may affect this mode (and contribute in fact to the measured value of its Q factor).

II. Acoustic and Electric Dissipation in Trapped Modes

Governing equations: We consider dissipation constituted by viscous damping and conductivity (the consideration of dielectric dissipation would have conduct to very similar formula except for the frequency dependence of the effect). The starting equations are the stress equation of motion, the linear constitutive equations accounting here for viscous damping and the Maxwell equations (in the quasi-electrostatic approximation).

$$T_{ij,i}=\rho\ddot{u}_j,$$

$$D_i=e_{ijk}S_{jk}+\varepsilon_{ik}E_k \qquad T_{ij}=c_{ijkl}S_{kl}-e_{ijk}E_k+\eta_{ijkl}\dot{S}_{kl}\ ,$$

$$J_i=\sigma_{ik}E_k \qquad \dot{D}_{i,j}=-\sigma_{ik}E_{k,j}\ , \qquad \mathrm{E_k}=-\Phi_{,k}\ ,$$

A. One dimensional thickness modes [12-13].

The Christoffel equation (1 D. thickness mode propagating along the normal **n** to an infinite plate) has now complex eigen-values and eigen-vectors $\bar{C}_{(i)}$, $\vec{U}_{(i)}$.

$$\left\{\left[C_{ijkl}n_jn_l+j\omega\eta_{ijkl}n_jn_l\right]+\left[\frac{\gamma_j.\gamma_k}{\varepsilon_{ij}n_in_j-j\dfrac{\sigma_{ik}n_in_k}{\omega}}\right]\right\}U_k=\frac{\rho\omega^2}{k^2}U_j$$

With $\gamma_k=e_{ijk}n_in_j.$

The wave number k and the coupling coefficients K are also complex numbers. Lee [6] has shown how the different kind of dissipation has influence on these quantities.

$$\bar{C}_{(i)}=\bar{c}_{(i)}+j\omega\bar{\sigma}_{(i)}+\frac{j}{\omega}\bar{\sigma}_{(i)}=\frac{\rho\omega_2}{k^2_{(i)}} \qquad K^2_{(i)}=\frac{\left[\gamma_kU^{(i)}_k\right]^2}{\bar{C}_{(i)}}\left[\frac{1}{\varepsilon_n-\dfrac{j}{\omega}\sigma_n}\right]$$

B. Tiersten's theory and dissipation.

The theory of "essentially thickness modes" [12-13] makes the assumptions that the displacements has thickness variations which are "essentially" similar to those of the 1 D modes of infinite plate, but also that they have lateral variations related to thickness variations and/or to the effects of the electrodes. This theory leads to a partial derivative equation governing the lateral dependence of the main displacement (noted u_1 by convention).

$$M'n\tilde{u}^n_{1,11}+P'n\tilde{u}^n_{1,33}+(\rho\omega^2-n^2\pi^2c^*/4h^2).\tilde{u}^n_1=(-1)(n-1)/24\rho\omega^2e_{26}V_0\exp(j\omega t)\Big/(c(1)n^2\pi^2) \quad (1)$$

The coefficients of this equation, M_n, P_n, C* and $C^{(1)}$ are either the 1 D stiffened elastic constant themselves or are functions of them, of the coupling coefficients and of other elastic, viscosity dielectric and conductivity constants of the crystal. So that the lateral components of the displacements are also complex. C* is either the stiffened elastic constant of the corresponding 1 D mode ($\overline{C}$) for the regions without electrodes or a value of this constant modified to account for the mass and electrical effects of the electrodes in the corresponding regions ($\hat{C}$). $C^{(1)}=C^*(1-K^2)$ is a pseudo ordinary elastic constant (C'_{66} for Y rotated quartz), ρ is the density, 2h the plate thickness, Vo is the forcing potential (by convention, zero outside of the electrodes). This equation was obtained [13] in transforming the displacement and the potential in order to replace the inhomogeneous boundary condition on the potential by a forcing term in the equations (electroded region only, Vo=0 elsewhere).

$$\Phi_e=-\frac{x_2 V_0\exp(j\omega t)}{2h}+\frac{e_{26}}{\varepsilon_{22}}u_{1e}-\frac{e_{26}}{\varepsilon_{22}}\frac{x_2}{h}u_{1e}(h)$$

$$u_{1e}=\hat{u}_{1e}-\frac{e_{26}x_2V_0\exp(j\omega t)}{2hC^{(1)}};\ with:\ \hat{u}_1=\tilde{u}_1.\sin(n\pi x_2/2h)$$

1) Short-circuit eigen modes: When V=0, $\hat{u}_1\equiv u_1$ in any region.

$$M'_n\ \tilde{u}^n_{1,11}+P'_n\tilde{u}^n_{1,33}+4\pi^2\rho\left[f2-\left(\frac{n^2C^*}{(4h)^2\rho}\right)\right]\tilde{u}^n_1=0 \qquad (2)$$

Since Mn, Pn and C* are complex quantities this equation separates into a real and an imaginary equation that can be solved for the real and the imaginary part of u_1. We make the coordinate transformations (taking respectively the real or the imaginary parts of Mn', Pn', C*) defined by:

$$X_1=\sqrt{\frac{\mathrm{Re}al(c^*)}{\mathrm{Re}al(M'_n)}}.\gamma.x_1\ \text{ or }\ X_1=\sqrt{\frac{\mathrm{Im}ag(c^*)}{\mathrm{Im}ag(M'_n)}}.\gamma.x_1=r\cos t$$

$$X_3=\sqrt{\frac{\mathrm{Re}al(c^*)}{\mathrm{Re}al(P'_n)}}.\gamma.x_3\ \text{ or }\ X_3=\sqrt{\frac{\mathrm{Im}ag(c^*)}{\mathrm{Im}ag(P'_n)}}.\gamma.x_3=r\sin t$$

With $\gamma^4=\frac{n^2\pi^2}{4h^4}$, It should be noticed that, most often, the coordinates systems are different for the real and the imaginary parts of the equation. These transformations lead, in each case, to an isotropic Helmoltz equation of the form:

$$\tilde{u}^n_{1,rr}+\frac{1}{r}\tilde{u}^n_{1,r}+\frac{1}{r^2}\tilde{u}^n_{1,tt}+A^*\tilde{u}^n_1=\Delta\tilde{u}^n_1+A^*\tilde{u}^n_1=0 \qquad (3)$$

The complete equation (transformed coordinates) is:

$$\Delta\tilde{u}_1+A^*\tilde{u}_1=(-1)^{(n-1)/2}\frac{2}{n\pi}\frac{f^2}{f^{*2}}\frac{e_{26}}{c^{(1)}}V_0\exp(j\omega t)$$

Where $A^*=\frac{n\pi}{2}\left(\frac{f2-f^*2}{f^*2}\right)$(real part) or $A^*=-\frac{n\pi}{2}$ (imag.part)

and $f^2_*=\mathrm{Real}\left(\frac{n^2C^*}{(4h)^2\rho}\right)$ or $\mathrm{Imag}\left(\frac{n^2C^*}{(4h)^2\rho}\right)$

These Helmoltz equations can be separated into:

$$r^2R''+rR'+R(r^2A^*-\mu^2)=0 \qquad (4)$$

$$T''+\mu 2T=0\quad \mu=m \text{ integer} \qquad (5)$$

In both cases, the solutions of (4) are, depending on the sign of A*:-The Bessel functions $J_m(kr)$, $Y_m(kr)$ with $k=\sqrt{|A^*|}$ when A* >0 -or the modified Bessel functions $I_m(kr)$, $K_m(kr)$ when A*<0. The solutions of equation (5) are the trigonometric functions cos mt and sin mt. The solutions of equations (4) are chosen to have convenient values at r=0 and eventually at infinity. Those of (5) are chosen considering the symmetries of the devices. We make the approximation that the imaginary part of the Tiersten equation has only imaginary solutions.

A resonator having an elliptical electrode with an axis ratio equal to $a_1/a_3=\sqrt{M'_n/P'_n}$, made on an infinite plate, gives simple symmetric (in x_1 and x_3) solutions containing only one order (m) of Bessel functions. The solutions are respectively for the electroded region and the unelectroded region:

$$\tilde{u}^{nm}_{1e}=.B^n_m J_m(\hat{k}^n_r.r)\cos mt+j.B'^n_m\ I_m(\hat{k}^n_i.r')\cos mt\ '$$

$$\tilde{u}^{nm}_{1l}=C^n_m K_m(\bar{k}^n_r.r)\cos mt+j.C^n_m.K_m(\bar{k}^n_i.r')\cos mt'$$

Fundamental mode of the overtone n and its excited symmetric anharmonics corresponds to m=0, but the other modes with m>0 can be excited by particular dispositions or by asymmetries). The coefficients B and C and the resonance frequencies are found in expressing the continuity of u_1 and of its normal derivative at one point of the electrode edge (the electrode is circular in the transformed coordinates).

For a resonator of finite extension, made on an elliptical plate respecting the same condition of axis ratio for the electrode and for the plate the solutions are now:

$$\tilde{u}^{nm}_{1e}=B^n_m.J_m(\hat{k}^n_r.r)\cos mt+j.B'^n_m\ I_m(\hat{k}^n_i.r')\cos mt$$

$$\tilde{u}^{nm}_{1l}=C^n_m\left[K_m(\bar{k}^n_r.r)\cos mt+jK_m(\bar{k}^n_i.r')\cos mt'\right]$$
$$+D^n_m.I_m(\bar{k}^n_r.r)\cos mt+j.D'^n_m.I_m(\bar{k}^n_i.r')\cos mt'$$

The symmetric eigen-modes of resonators using electrodes and/or plate and/or fixations having other (symmetrical) geometries can be expressed as series (infinite sums over m) of the preceding solutions.

$$\tilde{u}^n_{1e}=\sum_{m=0}^{\infty}B^n_m.J_m(\hat{k}^n_r.r)\cos mt+jB'^n_m\ I_m(\hat{k}^n_i.r')\cos mt'$$

$$\tilde{u}^n_{1l}=\sum_{m=0}^{\infty}C^n_m.K_m(\bar{k}^n_r.r)\cos mt+j.C'^n_m.K_m(\bar{k}^n_i.r')\cos mt'$$
$$+\sum_{m=0}^{\infty}D^n_m.I_m(\bar{k}^n_r.r)\cos mt+jD'^n_m.I_m(\bar{k}^n_i.r')\cos mt'$$

In this case, the continuity conditions and the boundary conditions are expressed at a discrete number of points respectively for the real and for the imaginary part of u (for example p points of the electrode edge and p points at the plate edge and a truncation of the series to p terms is made [14]). We obtain so, a homogeneous linear system of equations relating the 6p coefficients A, A', B, B', C and C'. To have solutions, the determinant of this system must vanish. This condition constitutes a frequency equation which has for solutions the eigen frequencies fr_q. The eigen modes are then

found as the solutions of the homogeneous system for the corresponding eigen frequencies $f_{np.}$ Each is constituted of p (or 2p) real terms and of p (or 2p) imaginary terms. They are noted as: $\tilde{u}_{1e}^{n1}, \tilde{u}_{1e}^{n2}, \ldots\ldots \tilde{u}_{1e}^{nq}$ and $\tilde{u}_{1l}^{n1}, \tilde{u}_{1l}^{n2}, \ldots\ldots \tilde{u}_{1l}^{nq}$. In the case of uniform dissipation and with non-dissipative boundary conditions, we have found that the eigen frequencies depend only of the real parts of the Tiersten equation and that the solutions for the imaginary part are not independent of the solutions for the real part of the equation. So that both solutions should be computed separately (we will see that they are proportional despite the fact that they are different solutions of different equations).

Forced modes: The forced modes are expressed as a linear combination of this eigen-modes that verify the complete equations (respectively for their real and imaginary parts).

$$\tilde{u}_{1*}=\left[\sum_n\sum_j H_r^{nj}\tilde{u}_{1r*}^{nj}+jH_i^{nj}\tilde{u}_{1i*}^{nj}\right] \text{ with } \tilde{u}_{1*}=\tilde{u}_{1e} \text{ or } \tilde{u}_{1\ell}$$

$$u_{1l}=\tilde{u}_{1l}\sin(n\pi x_2/2h),$$

$$u_{1e}=\tilde{u}_{1e}.\sin(n\pi x_2/2h)-\frac{e_{26}x_2V_0\exp(j\omega t)}{2hC^{(1)}}.$$

The solution is substituted in the complete equation (1) and then the coefficients Hr and Hi are computed using the orthogonality relation existing for the solutions of Helmoltz equations constituting the real and imaginary parts of the Tiersten equation.

$$H_r^{np}=(-1)(n-1)/2\frac{f^2}{(f^2-f_{np}^2)}\frac{4e_{26}V_0\exp(j\omega t)}{n^2\pi^2c_*^{(1)}}\frac{\iint_{Se}\tilde{u}_{1*}^{np}dS}{\iint_{St}\left(\tilde{u}_{1*}^{np}\right)^2dS}$$

$$H_i^{np}=-(-1)(n-1)/2\frac{f^2}{\hat{C}_i.\gamma^2}\frac{4e_{26}V_0\exp(j\omega t)}{n^2\pi^2c_i^{(1)}}\frac{\iint_{Se}\tilde{u}_{1i}^{np}dS}{\iint_{St}\left(\tilde{u}_{1i}^{np}\right)^2dS}$$

In which only respectively the real part or the imaginary parts of f^2*, $C^{(1)}$, and u1 are considered

Electrical response. The usual potential is:

$$\Phi_e=\frac{x_2V_0\exp(j\omega t)}{2h}+\frac{e_{26}}{\varepsilon_{22}}u_{1e}-\frac{e_{26}}{\varepsilon_{22}}\frac{x_2}{h}u_{1e}(h)$$

The approximate constitutive relation for D2 is:

$$D_2=e'_{26}u_{1,2}-\varepsilon_{22}\Phi_{,2}$$

The current and the admittance are:

$$i=-\iint_{Se}(\dot{D}_2+J_2)dS \text{ and } Y=-\frac{1}{V_0\exp(j\omega t)}\iint_{Se}\left(\dot{D}_2+J_2\right)dS$$

When there are no losses, k'^2 and u_1 are real and $\sigma_{22}=0$, we express Y in function of the dynamic capacitance of the motional arms

$$Y=j\omega C_0+j\omega\sum_n\sum_p\frac{\omega_{np}^2}{(\omega_{np}^2-\omega 2)}C_{np}$$

$$Y=j\omega\left[\frac{\varepsilon_{22}Se}{2h}(1+k2)-\sum_n\sum_p\frac{\varepsilon_{22}8k'^2}{2h\,n^2\pi^2}\frac{f^2}{(f^2-f_{np}^2)}\frac{\left(\iint_{Se}\tilde{u}_1^{np}dS\right)^2}{\iint_{St}(\tilde{u}_1^{np})^2dS}\right]$$

With $k'^2 \# K^2(1+K^2)$. Therefore, that, without losses, the elements of the equivalent scheme is:

$$C_{np}=\frac{\varepsilon_{22}.8k'^2}{2h.n^2.\pi^2}\frac{\left(\iint_{Se}\tilde{u}_1^{np}dS\right)^2}{\iint_{St}\left(\tilde{u}_1^{np}\right)^2dS} \qquad L_{np}=\frac{1}{C_{np}.4\pi^2f_{np}^2}$$

$$C_0=C_Z-\sum_n\sum_p C_{np}\cong\frac{\varepsilon_{22}^SSe}{2h}; \quad C_z=\frac{\varepsilon_{22}^SSe}{2h}(1+k2)=\frac{\varepsilon_{22}^TSe}{2h}$$

When the losses are considered, the admittance Y is no more purely imaginary; it contains two real contributions due to the losses.

$$Y=\frac{1}{R_p}+j\omega C_0+\sum_{np}Y_{np}^{(reactive)}+\sum_{np}Y_{np}^{(losses)}$$

With $\frac{1}{R_p}=\frac{\sigma_{22}.S_e}{2h}$

When the losses are small, the imaginary (reactive) part of Y_{np} (and C_{np} and L_{np}) is essentially those of the real case. In other cases they can be computed from:

$$\mathrm{Im}ag(Y_{np})=-\omega.\frac{\varepsilon_{22}8.\mathrm{Re}al(k'^2)}{2h\,n^2\pi^2}\frac{f^2}{(f^2-f_{np}^2)}\frac{\left(\iint_{Se}\mathrm{Re}al(\tilde{u}_1^{np})dS\right)^2}{\iint_{St}(\mathrm{Re}al(\tilde{u}_1^{np}))^2dS},$$

The resistance and the Q factor of the motional arm are obtained from Real(Y_{np}): R_{np}= 1/Real(Y_{np}) and Q=L_{np} ω_{np}/R_{np} This leads to the equivalent scheme represented figure 5.

III. COMPUTED RESULTS.

Using the constants of quartz and the viscosity and conductivity given by Lamb and Richter [2], we have computed the mode shape and the equivalent scheme of several AT quartz resonators. The calculations concerning the imaginary part of the displacement are numerically difficult due to the very large coefficients of the modes (table II). As previously indicated the solution of the homogeneous system of the boundary and continuity conditions is made separately for the real and imaginary part of the displacement. This results of the fact that with uniform dissipation and non-dissipative boundary conditions the imaginary part of u1 is proportional to the real part everywhere.

Example 1: AT quart resonator using an elliptical electrodes and an elliptical plate (2h=0.2mm, R=1.0%, Electrode Ellipt. 2ax1=6mm, 2ax3=4.74mm, finite plate ellipt. 2ax1l=13mm, 2ax3l=10.27mm). Fixation in the x direction along a segment. The main complex coefficients of the Tiersten equation are given in table I. The coefficients of the truncated series (6 terms) of the first eigen-mode are given in table II.

TABLE I. MAIN COMPLEX COEFFICIENTS OF THE TIERSTEN EQUATION

M'n	= 0.10984507D+12 +j* 0.18271516D+06
P'n	= 0.68587457D+11 +j* 0.39181461D+05
Cpe	= 0.28471195D+11 +j* 0.34950433D+05 (modif. stiffnd const.)
Cbar	=0.29239901D+11 +j* 0.35663721D+05 (stiffened constant)
K2	= 0.77595044D-02 -j* 0.94636229D-08

TABLE II. COEFFICIENTS OF THE EIGEN MODE 1 (REAL & IMAGINARY)

coefficients A_{1i} & A'_{1i} (I=1TO 6)					
I=1	-0.52022170D+01	0.53719042D+00	2	0.12820175D-02	0.10000000D+01
3	0.36829472D-02	0.78917095D+00	4	0.20080049D-01	0.49505857D+00
5	0.14451582D+00	0.21819576D+00	6	0.10000000D+01	0.50495125D-01
coefficients B_{1i} & B'_{1i}					
1	-0.70881727D+02	-0.56869466D+23	2	0.35278218D-02	0.11968953D+24
3	0.10015084D-03	-0.58248722D+23	4	0.10733599D-05	0.38779197D+23
5	0.68289043D-08	-0.65076774D+22	6	0.46231278D-10	0.29191850D+22
coefficients C_{1i} & C'_{1i}					
1	-0.43079697D-04	0.24025999D+09	2	0.82815362D-04	0.94112584D+09
3	0.13701608D-03	0.19338668D+10	4	0.29831394D-03	0.32086499D+10
5	0.73987943D-03	0.32330180D+10	6	0.14908621D-02	0.18056319D+10

The shape of the real and imaginary part of the eigen modes (normalized so that (u_1*(0,0)=1) are represented in figure 6. They are obviously identical so that the imaginary part of u_1 is proportional everywhere to the real part. The coefficients of proportionality are given (for the forced modes) by the ratio of the H^*_{np} coefficients.

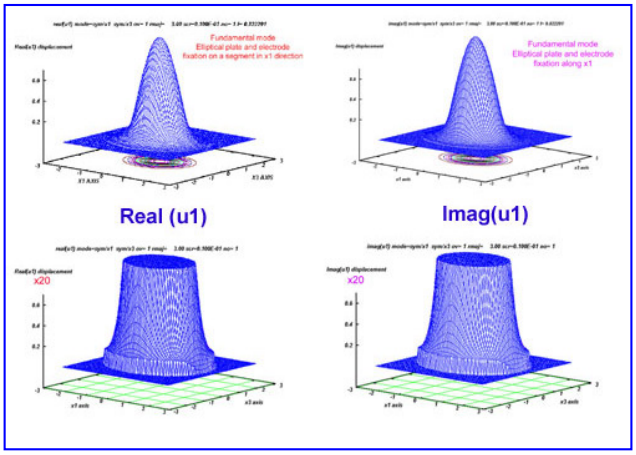

Figure 6. Real and imaginary part of the eigen-modes (normalised to 1 and details (x20) to observe u_1 near the free part of the edge or the fixation)

Example 2: AT quartz with a circular electrode on an infinite plate. (2h=0.2mm, Φe=6mm, mass loading 1%). This device has three modes, the resonance frequency of the first one is fr_1=8.218382MHz. The corresponding eigen mode (real part or imaginary part) is represented on figure 7. The element of the equivalent scheme are given in table III.

TABLE III. EQUIVALENT SCHEME OF THE FUNDAMENTAL MODE

C11 (Motional C.)	30.5 fF	L11 (motional L)	0.122 H
R11 (serial R)	0.39 Ω	Q11 (Qfactor arm 11)	0.16 E+7
Co (// Capacitance)	5.628 pF	Rp (// Resistance)	0.21E+14 Ω

The computed value of the serial resistance is less accurate than the motional inductance (integration of very small quantities). It is much smaller than the experimental ones. The computed Q factor is much higher than the experimental values that are the order of 80.000 with a very large plate (15mm diameter). It appears thus that the calculations made with uniform dissipation and non-dissipative boundary conditions (u_1=0 or $\partial u_1/\partial n$=0) could not represent the main source of dissipation in fundamental mode resonators. This one is quite certainly constituted by energy leakage at the fixation.

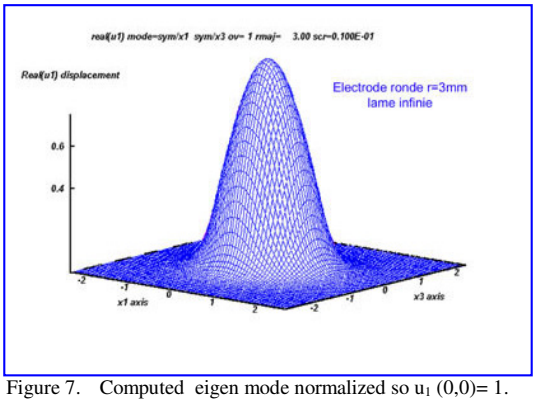

Figure 7. Computed eigen mode normalized so u_1 (0,0)= 1.

IV. CONCLUSION

The calculations made considering viscous losses and conductivity for fundamental modes AT quartz resonators give Q factors that are close to what is considered as the intrinsic limit for quartz resonators but that are, by more than one order of magnitude, larger than the experimental values. This indicate that in such cases a much more important cause of dissipation exist. The experiments have indicated that energy leakage via the fixations of the device is probably the dominant factor in this case. Such a mechanism should be investigated using numerical simulations using dissipative boundary conditions and, much probably, considering progressive waves to evaluate further its importance in high performance devices

References:

[1] A.W. Warner. Bell System Technical Journal Sept. 1960 p.1193-1217.
[2] J. Lamb, J. Richter. Proc. Roy. Soc. v. 293A, p.479-492. (1966).
[3] A. Glowinski. Annales Telecom. v.27, n°3-4, p.147-158 (1972).
[4] A.Ballato. "Doubly rotated plate vibrators" in Physical Acoustics v.13. W.P.Masson, R.N.Thurston editors.Academic Press (1977).
[5] R. Holland, E.P. Eernisse. Design of resonant Piezoelectric devices M.I.T. Press (1968).
[6] P.C.Y. Lee, N. Liu, A.Ballato. IEEE Trans. Ultrason, ferroel. Freq. Control. v.51 p.52-62 (2004).
[7] J. Detaint, B. Capelle, A. Zarka, D. Cochet-Muchy. Proc.9th European Frequency and Time Forum (EFTF) p.289-296. (1995).
[8] R. Shane Fazzio. Ultrasonics v. 45 p.196-207 (2006).
[9] A. Zarka, B. Capelle, Y. Zheng, J. Détaint, J. Schwartzel. Proc. 42nd Annual Frequency Control Symp.p.85-92 1988.
[10] Y.Zheng, A.Zarka, B.Capelle, J.Detaint, J.Schwartzel. Acta Cryst. v.A45, p.275-285 (1989).
[11] B. Capelle, J. Detaint, J. Schwartzel, A. Zarka, Y. Zheng,, C.Joly. Proc. 5th EFTF p.41-49. (1991).
[12] H.F. Tiersten J. Acoust. Soc. Am. v.57, p.667-681 (1975)
[13] D.S. Stevens, H.F. Tiersten., J. Acoust. Soc. Am. v.79 p.1811-1826 (1986).
[14] J. Detaint, J.Schwartzel, C.Joly, B.Capelle, A.Zarka, E.Philippot. Proc. 1992 IEEE Int Frequency Control Symposium p.639-647. (1992)

..